Structure of thin diamond films: A ^1H and ^{13}C nuclear-magnetic-resonance study

M. Pruski, D. P. Lang, and Son-Jong Hwang
Ames Laboratory and Department of Chemistry, Iowa State University, Ames, Iowa 50011

H. Jia and J. Shinar
Ames Laboratory and Department of Physics and Astronomy, Iowa State University, Ames, Iowa 50011
(Received 2 August 1993; revised manuscript received 4 January 1994)

The ^1H and ^{13}C nuclear magnetic resonance (NMR) of thin diamond films deposited from naturally abundant (1.1 at. %) as well as 50% and 100% ^{13}C-enriched CH_4 heavily diluted in H_2 is described and discussed. Less than 0.6 at. % of hydrogen is found in the films which contain crystallites up to ~ 15 μm across. The ^1H NMR consists of a broad 50–65-kHz-wide Gaussian line attributed to H atoms bonded to carbon and covering the crystallite surfaces. A narrow Lorentzian line was only occasionally observed and is found not to be intrinsic to the diamond structure. The ^{13}C NMR demonstrates that $>99.5\%$ of the C atoms reside in a quaternary diamondlike configuration. ^1H-^{13}C cross-polarization measurement indicates that, at the very least, the majority of ^{13}C nuclei cross polarized by ^1H, i.e., within three bond distances from a ^1H at a crystallite surface, reside in sp^3 diamondlike coordinated sites. The ^{13}C relaxation rates of the films are four orders of magnitude faster than that of natural diamond and believed to be due to ^{13}C spin diffusion to paramagnetic centers, presumably carbon dangling bonds. Analysis of the measured relaxation rates indicates that within the ^{13}C spin-diffusion length of $\sqrt{DT_1} \sim 0.05$ μm, these centers are uniformly distributed in the diamond crystallites. The possibility that the dangling bonds are located at internal nanovoid surfaces is discussed.

I. INTRODUCTION

The extreme qualities of diamond (density, hardness, chemical inertness, high electrical resistivity, and thermal conductivity) have opened pathways for numerous technological applications of this material in the areas of microelectronic circuitry, tribology, coatings, and optics.[1,2] A process of synthesizing diamond at high temperatures and pressures, where diamond is the stable form of carbon, was developed nearly four decades ago,[3] and parallel efforts for growing diamond at lower pressures were also underway. The growth of thin diamond films at low pressures, where diamond is a metastable form of carbon, using thermally assisted chemical vapor deposition (CVD) of CH_4 heavily diluted in H_2 has since been investigated extensively.[1,2,4,5] Still, the detailed picture of the chemical structure and electronic properties of the films and their native defects is incomplete.[6–9] Similarly, the role of hydrogen, a ubiquitous impurity within the CVD films, and its possible bonding sites are not completely understood.[10] In this study, nuclear magnetic resonance (NMR) of ^1H and ^{13}C and electron spin resonance (ESR) were used in conjunction with scanning electron microscopy (SEM) and Fourier-transform infrared spectroscopy (FT-IR) to examine natural and ^{13}C-enriched CVD diamond films grown on a silicon wafer substrate.

Previous NMR studies of thin diamond films and diamond powders have been reported by Gleason and coworkers,[7–9,11] and Henrichs *et al.*[12] Other studies of isotopically enriched diamonds were reported by Banholzer and Anthony.[13] The NMR has shown that the H content is typically 0.1–0.5 at. %,[8,11] that the H atoms predominantly "decorate" the crystallite surfaces,[11] and that the ^{13}C relaxation rates are much faster than those found in natural diamonds.[12] This study confirms some of these earlier conclusions, but it also provides new insight into the nature of the polycrystalline films: (i) the narrow $\sim$5-kHz-wide Lorentzian ^1H NMR line typically observed on top of the main $>$50-kHz-wide Gaussian line and attributed to rotating methyl groups,[9] is found to represent hydrogen that is not intrinsic to the diamond films studied in this work. (ii) The ^{13}C NMR of the ^{13}C-enriched samples indicates that at least 99.5% of the C atoms are in a quaternary diamondlike environment. The ^{13}C cross polarization by ^1H nuclei indicates that, to within the CP signal-to-noise ratio, all of these carbons which are not more than 2–3 lattice spacings away from a H atom, are in a similar diamondlike configuration. (iii) In agreement with previous studies of synthetic diamonds,[12] we find that the ^{13}C relaxation rates in CVD diamond films are much faster than found in natural crystals. However, analysis of the measured rates in naturally abundant and ^{13}C-enriched CVD's indicates that the dangling bonds responsible for relaxation are homogeneously distributed in the diamond crystallites. This conclusion is significant, and its interesting consequences are discussed below.

II. EXPERIMENT

A. Samples

The films were grown by flowing a mixture of $\sim 99.5\%$ H_2 and $\sim 0.5\%$ CH_4 at a pressure of $\sim$50 Torr through a tungsten filament heated to $\sim$2000 °C onto a silicon wafer substrate heated to 850 °C. The growth rate of the films

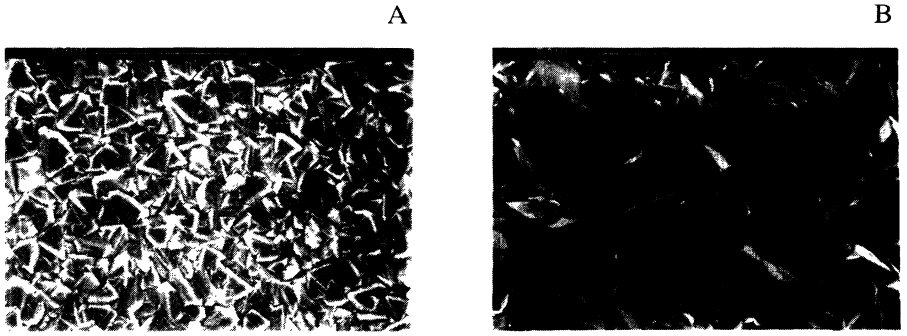

FIG. 1. Scanning electron micrographs of diamond films *A* and *B*.

was ~ 0.5 μm/h. Following the deposition process, the silicon substrate was dissolved in HF to yield free-standing films. About 15 mg of film *A* was grown over 13 h using 100% ^{13}C-enriched methane at a flow rate of ~ 200 SCCM (cubic centimeter per minute at STP); film *B* was grown for 80 h from natural ^{13}C-abundant CH_4 at the same flow rate to yield ~ 70 mg. Film *C* was grown over 21 h under the same conditions using 50% ^{13}C-enriched methane. SEM images of films *A* and *B* are shown in Fig. 1. Note that the top crystallites of film *B* are much larger than those of film *A*, consistent with the observations[9,11,14] that the crystalline size increases with the distance (i.e., growth time) from the substrate.

B. NMR

Proton NMR spectra at 100–300 K were acquired using a home-built spectrometer operating at a Larmor frequency of 250 MHz. Spin-temperature inversion with signal subtraction on alternate scans in the averaging process[15] was used to eliminate baseline distortions from the NMR signal. Using quadrature detection, 2-μs dwell time, and a 10-s delay between scans, 10^3–10^4 free-induction decays (FID's) were averaged to yield each spectrum.

^{13}C spectra were obtained at room temperature using another home-built spectrometer operating at Larmor frequencies of 100.06 MHz for ^{1}H and 25.15 MHz for ^{13}C. The ^{13}C spin-lattice relaxation time T_1 for each diamond film was measured without magic angle spinning (MAS) using the Bloch decay progressive saturation technique.[16] Five hundred FID's were acquired using spin-temperature inversion for several (9–15) different delays ranging from 1 to 1000 s. The MAS spectra were acquired using a double-tuned, single-coil probe equipped with a modified Shoemaker-Apple type magic angle spinner.[17] For the 100% ^{13}C-enriched film *A*, the extremely weak ^{1}H-^{13}C cross-polarization (CP) MAS spectrum was also measured. The Hartmann-Hahn condition was established using an rf field of 60 kHz for a static sample of adamantane. The proton rf field was kept at the same level during the high-power ^{1}H-^{13}C decoupling. In this experiment 80 000 scans were acquired using a delay of 2 s, a 2-ms contact time, 2-K data points in each quadrature channel, 5-μs dwell time and a sample spinning rate of 4.5 kHz. All NMR spectra are reported from tetramethylsilane, using the δ scale, with negative values being upfield.

C. FT-IR

The infrared spectrum of film *B* was recorded on a modified Nicolet 710 FT-IR spectrometer equipped with a Harrick diffuse reflectance accessory and a mercury cadmium telluride detector. The spectrum was normalized using a mirror background standard and was baseline corrected.

D. ESR

Electron spin resonance spectra were obtained using a commercial Bruker ESR 200 spectrometer, with a sensitivity of $\sim 10^{11}$ spins/G. The ESR spin densities were determined by comparing with known diphenylpicrylhydrazyl standards, sealed in evacuated quartz tubes.

III. RESULTS AND DISCUSSION

A. ^{1}H NMR line shape

The typical ^{1}H NMR spectrum of the diamond films measured in this work (shown in Fig. 2 for film *B*) consists of a broad Gaussian line of $\sim 65 \pm 5$ kHz full-width at half-maximum (FWHM). Similar Gaussian lines of widths 50 ± 5 and 65 ± 5 kHz were observed in samples *A* and *C*, respectively. The total hydrogen content in films *A* and *B* *(vide infra)* and the ^{1}H NMR line-shape parameters are given in Table I. In agreement with previous reports,[8,11] the H contents were only a fraction of 1 at. %. We first note that due to this low abundance of hydrogen, the relatively broad linewidth, and the small 15–70-mg samples, corresponding to less than 5×10^{18} ^{1}H spins, the accurate measurements of the ^{1}H NMR line shapes and

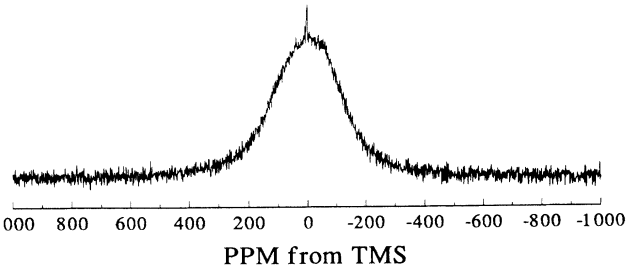

FIG. 2. Solid-state ^{1}H NMR spectrum of diamond film *B*. The broad Gaussian component represents densely packed hydrogen bonded to carbon on crystallite surfaces.

TABLE I. NMR and ESR parameters of the thin diamond films: percent ^{13}C enrichment, % ^{13}C; total atomic percent hydrogen, at. % ^1H_T; full width at half-maximum of the ^1H NMR spectrum, FWHM; proton spin density, N_H; average surface area per gram, S; estimated average diamond crystallite size, a; electron spin density, N_e; average distance between radicals if confined to the surface, R_{es}; average distance between radicals if they are distributed uniformly within the bulk, R_{ev}.

Sample	film A	film B
% ^{13}C	100	1.1
at. % ^1H_T	0.56	0.15
FWHM (kHz)	50	65
N_H (spins/g)	2.6×10^{20}	7.3×10^{19}
S (nm^2/g)	8.7×10^{18}	2.4×10^{18}
a (μm)	0.2	0.7
N_e (spins/g)	3.6×10^{17}	4.4×10^{17}
N_e (ppm)	7.8	8.8
R_{es} (nm)	4.9	2.3
R_{ev} (nm)	9.3	8.6

hydrogen concentrations were challenging. In order to eliminate background NMR signal we used a hydrogen-free probe that was purged with dried air during the measurements. The diamond samples were placed in 5-mm-o.d. cylindrical NMR tubes, evacuated for one hour at 10^{-5} Torr and 140 °C to remove weakly bound contaminants (including moisture), and sealed prior to the NMR measurements. A background signal was measured using an empty reference tube prepared under identical conditions and its ^1H spectrum was subtracted to yield the final ^1H spectrum of the diamond film.

The ^1H NMR linewidth and line shape is clearly attributable to rigid dipolar coupled proton spins in a densely packed environment. If the H atoms were homogeneously distributed within the diamond, a linewidth of only a few hundred Hz could be expected for the concentrations of spins measured in this work *(vide infra)*. Assuming the homonuclear proton-proton dipolar coupling to be the dominant line-broadening mechanism, and specifically larger than the broadening associated with paramagnetic center-nuclear dipolar interaction and shielding anisotropy, the Van Vleck equation can be used to estimate the second moment of the NMR line[18]

$$\langle \Delta H^2 \rangle = \frac{1}{N} \sum_{i,j} \left\{ \left[\frac{9}{20} \right] \frac{\gamma^4 \hbar^2}{r_{ij}^6} \right\} , \quad (1)$$

where γ, $\hbar$, and r_{ij} have their usual meanings and N is the number of protons occupying inequivalent positions in the repeating structure unit. For rigid protons, i.e., those with correlation time for motion $t_c \gg (\delta\nu)^{-1}$, the NMR line shape can be approximated by a Gaussian curve with a FWHM given by[18]

$$\delta\nu \approx 2.36\sqrt{\langle \Delta H^2 \rangle} . \quad (2)$$

Based on crystallographic data[19,20] and the SEM images presented in this work (Fig. 1), we assume that (100), (110), and (111) are the most prominent orientations in the diamond films studied. Using Eqs. (1) and (2) and assuming that hydrogen stabilizes these surfaces, ~70-, ~40-, and ~30-kHz linewidths should be observed for these orientations, respectively. A superposition of these lines can be easily used to fit the broad portion of the ^1H NMR spectra, which suggests that the model of hydrogen stabilizing the (100), (110), and (111) surfaces by forming a monolayer of C-H species is reasonable. The change in surface texture between films A and B, visible in the SEM images (Fig. 1), results from differences in the deposition time and film thickness.[9,11,14] Due to the low signal-to-noise ratio and the number of parameters involved, the numerical decomposition of the ^1H NMR spectra is only qualitative: although assuming a single crystal orientation does not allow us to describe the broad resonance, the contributions from different crystal orientations cannot be quantitatively determined from such analysis. We note, however, that for two of the three samples studied a 65±5-kHz linewidth was measured which strongly indicates that the (100) is the dominant surface.

In earlier studies[8,9,11] a narrow Lorentzian ^1H line (2–6-kHz wide) was also observed. This component, due to a small fraction of the hydrogen, suggested the existence of another environment with weaker dipolar coupling, either due to mobility or isolation from neighboring spins. Gleason and co-workers[9,11] suggested that rotating CH_3 groups on the crystallite surface were responsible for this component. Indeed, it had been postulated earlier that radicals, in particular CH_3 and H, control the gas-phase chemistry of CVD diamond growth,[21] and, therefore, could play an important role as propagating units and/or lattice terminating species.

A narrow 2–6-kHz resonance was also found in some of the spectra obtained in this work. However, based on the quantitative measurements described above, the narrow resonance could not be unambiguously ascribed to hydrogen in diamond films. As was mentioned earlier, quantifying the hydrogen in the diamond films required precise monitoring of the residual background signal originating from the probe and the glass tubes. This signal consisted of a narrow peak superimposed on a broad feature and could not be completely eliminated by heating the sample tubes under vacuum and purging the probe with dry air. Since its intensity remained comparable with that of diamond films, a residual narrow feature, representing between 0 and 10% of the total intensity, remained in some spectra after background subtraction, either as a small peak (see Fig. 2) or a "hole." Despite several attempts we were unable to establish that the existence of the narrow resonance line was related to hydrogen intrinsic to diamond films studied in this work. We also note that based on the experiments performed in this study we see no feasible hypothesis that would explain the existence of such a narrow feature in the spectra. One configuration involving isolated hydrogen in diamonds was considered in our recent ESR work,[6] where dangling-bond-H centers embedded in the vacant carbon site of the tetrahedral diamond network were postulated. However, hydrogen atoms involved in such centers would not be detectable by NMR due to low concentration (<1 ppm) and paramagnetic line broadening.

A hypothesis involving rotating CH_3 groups is also unlikely. The width of an NMR line for a given system of

dipolar coupled spin-$\frac{1}{2}$ nuclei depends not only on the local nuclear configuration but also on the motion of the nuclei.[22] In particular, the ^{1}H NMR linewidth of a CH_3 group rotating around its C_3 axis at room temperature ($\nu_{rot} > 100$ kHz) approaches $\sim$20 kHz, which is half of the width for the case of a rigid lattice. Typically, this narrowing of the CH_3 resonance occurs at temperatures between -170 and 120 °C.[23] Thus, if the $\sim$5-kHz resonance observed in this work was due to surface CH_3 groups, a more isotropic motion would have to be assumed. This type of motion is highly improbable on the diamond surface at room temperature. Also, the presence of CH_3 groups could not be unambiguously detected using FT-IR. An FT-IR analysis performed on film *B* (Fig. 3) shows absorption in both the one and two phonon areas of the spectrum, as well as in the C-H stretch region. While absorption in the two-phonon range (1333–2666 cm^{-1}) is expected for a pure diamond sample, absorption in the one phonon range (<1330 cm^{-1}) is attributed to impurities in the diamond lattice that disrupt its translational symmetry.[24–26] The presence of a resolved peak at $\sim$2830 cm^{-1}, observed within the C-H stretch region of the FT-IR spectrum (2800–3000 cm^{-1}), is attributed to a single C-H bond stretch vibration on a fully relaxed (111) diamond surface.[27,28]

Since no evidence of adsorbed water is found in the IR spectrum, its presence is also unlikely. Furthermore, we considered the existence of residual concentration of hydrogen gas trapped inside the crystallites, and exhibiting restricted thermal reorientation. This possibility was excluded by performing a variable temperature line-shape measurement for sample *B* between -170 °C and room temperature, which showed that below ~ -70 °C the Lorentzian component broadened and could not be distinguished from the Gaussian part even when background signal was present in the spectrum. Finally, the possibility of methane molecules remaining trapped in the microvoids of crystallites was investigated. To that end we prepared a diamond film using a mixture of H_2 and deuterated methane CD_4, but observed no change in the NMR spectra.

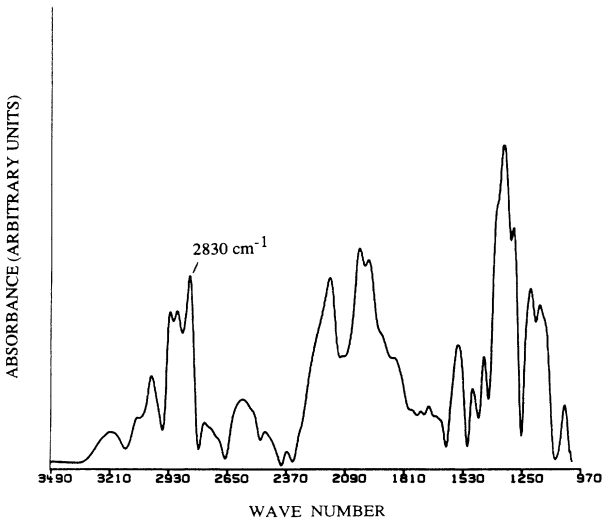

FIG. 3. FT-IR spectrum of film *B* over the absorption range 1000–3500 cm^{-1}.

In summary, at least 95% of the ^{1}H NMR intensity detected in this work originates from strongly coupled H atoms localized on the crystallite surfaces. The narrower NMR component observed in some spectra cannot be attributed to hydrogen intrinsic to diamond films or representing an invariant part of their structure.

B Hydrogen content

Using ^{1}H NMR spectroscopy for measuring hydrogen concentration implies that all of the proton spins are detected in the NMR experiment and that the intensity of the FID at $t=0$ is correctly determined. In the pulsed NMR experiment, the first few microseconds of the signal following a transient rf excitation cannot be observed due to probe ringdown and receiver deadtime (6 μs in our spectrometer). We used a linear backwards prediction method to recover the initial part of the FID. After subtracting the background, the resulting spectra were compared to that of a known quantity of water, to yield the H concentrations N_H given in Table I.

Also listed in Table I are other parameters of samples *A* and *B* measured or determined in this work: the calculated average surface area per gram *S*; average crystallite size *a*; unpaired electron spin densities N_e obtained from ESR; and average distances between unpaired electrons R_{es} and R_{ev} calculated assuming uniform distribution on the surface or in the bulk, respectively. For the calculation of *S*, we assumed that hydrogen decorates a (100) crystal face, which yields a surface density $D_s \cong 3\times 10^{15}$ protons per cm^2. Subsequently, *S* is estimated using the formula $S=N_H/D_S$, from which the average crystallite size is derived assuming a cubic shape. The electron-electron distances were found using the formulas $R_{es}=\sqrt{S/N_e}$ and $R_{ev}=1/(dN_e)^{1/3}$ where $d=3.51$ g/cm^3 is the diamond density. The ESR data will be used later in the analysis of ^{13}C spin-lattice relaxation.

The NMR spin count results show that the hydrogen concentration in diamond film *A* is higher than in film *B*. Assuming that the hydrogen essentially covers the crystallite surfaces, the previous result is in agreement with the SEM images in Fig. 1 which show that the top of diamond film *A* consists of smaller diamond particles. We also observe that for both samples the crystallite sizes *a* calculated above are considerably smaller than those observed on the surfaces of the films, which are several μm across (Fig. 1). This is probably due to a distribution of crystallite sizes in the diamond films with generally larger crystallites growing at greater heights from the silicon substrate.[9,11,14] Also, as suggested earlier, the existence of internal surfaces within the crystallites should not be excluded. Thus, the values of *a* given in Table I should only be considered as the *lower limit* of the average crystallite size. We will refer to these values below in the discussion of spin diffusion and relaxation.

C. ^{13}C MAS NMR

^{13}C MAS direct excitation (Bloch decay) spectra of diamond films *A* and *B* are presented in Figs. 4(a) and 4(b),

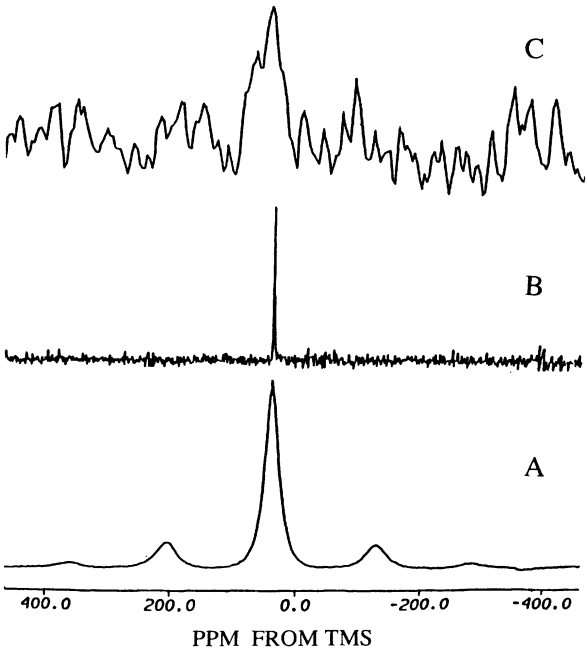

FIG. 4. ^{13}C MAS NMR spectra of the diamond films: (A) Bloch decay spectrum of 100% ^{13}C-enriched sample *A*; (B) Bloch decay spectrum of sample *B* with natural abundance of ^{13}C nuclei; (C) CP/MAS spectrum of sample *A* after 80 000 scans.

respectively. A single isotropic peak centered at 36±2 ppm is observed, characteristic of carbon in the tetrahedrally symmetric environment of natural diamond[12,29] and diamond films studied previously.[7,8] For the ^{13}C-enriched sample [Fig. 4(a)] a central peak (~600 Hz FWHM) is accompanied by spinning sidebands resulting from ^{13}C-^{13}C homonuclear dipolar coupling which is only partly eliminated by MAS at 4.5 kHz (a dipolar powder pattern width of ~10 kHz was measured in a static experiment). At least 99.5% of the carbon in sample *A* is determined to reside in an sp^3 diamondlike configuration. The static spectrum of diamond film *B* (not shown) exhibited a linewidth of ~300 Hz (FWHM) which resulted from residual chemical shift anisotropy and magnetic susceptibility. This spectrum was narrowed by MAS to ~75 Hz [Fig. 4(b)]. We note the absence of a shoulder at ~30 ppm, which was observed in a MAS spectrum of a diamond film studied recently by Lock, Maciel, and Johnson[30] using dynamic nuclear polarization (DNP) NMR.

D. ^{13}C CP/MAS NMR

In the ^{13}C CP/MAS experiment, the polarization of carbon nuclei is achieved indirectly via the ^{1}H-^{13}C dipolar interaction, and the obtained spectra represent primarily those ^{13}C spins that are less than three bond distances away from the nearest proton. The very low H content in diamond films severely reduced the fraction of ^{13}C spins that could be polarized in this experiment. However, after 80 000 cross-polarization scans we were able to develop a spectrum from the ^{13}C-enriched sample *A* [Fig. 4(c)]. The single distinguishable spectral feature is a resonance centered at 36±5 ppm, which is broader than a corresponding line in the Bloch decay spectrum of Fig. 4(a). A similar ^{13}C spectrum was observed earlier using the DNP/CP/MAS technique.[30] This important result confirms that the majority of ^{13}C spins in film *A* which are polarized by hydrogen reside in sp^3 diamondlike coordinated sites. Furthermore, it shows that the reconstruction of the diamond surface, which would result in a graphiticlike structure (a mixture of hybrid sp^2 bonds and unhybridized *p* orbitals[10]), is prevented by atomic hydrogen surrounding the diamond during the thermally assisted CVD synthesis.

E. ^{13}C longitudinal relaxation

^{13}C relaxation times T_1^c were measured with the progressive saturation method, as described in Sec. II, using nonspinning samples to prevent the hindrance of spin diffusion among ^{13}C nuclei by MAS. The T_1^c values of 8±1, 67±5, and 17±2 s were measured for samples *A*, *B*, and *C*, respectively. By comparing the intensities of the ^{13}C NMR measured in this experiment to that of a calibrated standard we have determined that within the accuracy of such measurement (±20%) all of ^{13}C nuclei in samples *A*, *B*, and *C* were detected in the relaxation studies. Below, we consider possible mechanisms for longitudinal relaxation in diamond films.

We first note that the T_1^c values measured in this work are four orders of magnitude shorter than those reported previously for natural diamonds.[12] This result, and the high electron spin counts seen in the ESR measurement (Table I), strongly suggest that the interaction of ^{13}C spins with paramagnetic centers is the primary relaxation mechanism in thin diamond films. In the analysis of this relaxation mechanism it is convenient to introduce several parameters. The diffusion barrier δ is the distance from the paramagnetic site outside of which the spin-diffusion coefficient D is constant, and inside of which $D=0$, as mutual spin-flip processes become impossible due to the large differences in the resonance frequencies of neighboring nuclei. A pseudopotential radius ρ describes a sphere around the paramagnetic site within which proton relaxation is dominated by the electron-proton interaction. Several limiting cases for the effective paramagnetic relaxation are described in the literature,[31–37] depending on the relative magnitudes of δ, ρ, and the average distance between paramagnetic sites R_e. There are three possibilities: (1) $\rho<\delta$ [complete, or fast, spin diffusion (CSD)], (2) $R_e>\rho>\delta$ [limited spin diffusion (LSD)], (3) and $\rho>R_e$ [vanishing spin diffusion (VSD)]. For a homogeneous system the relaxation function $M(t)$ is given by

$$M(t)=M_0\{1-\exp[-(t/T_1^c)^n]\}\ , \tag{3}$$

where M_0 is the equilibrium magnetization. For the present discussion we only note that for CSD and LSD the relaxation function $M(t)$ is exponential in time ($n=1$), with a relaxation time T_1^c proportional to $(N_eD)^{-1}$. In the VSD limit, however, $n=0.5$ is expect-

ed. To determine which of the limiting cases applies to diamond films we first consider the pseudopotential radius ρ. From relaxation theory[18]

$$\rho=(A_e/D)^{1/4} \tag{4}$$

with

$$A_e=0.3(\gamma_e\gamma_n\hbar)^2\left\{\frac{T_{1e}}{1+T_{1e}^2\omega_n^2}\right\}, \tag{5}$$

where γ_e and γ_n are the magnetogyric ratios of the electrons and nuclei, respectively, ω_n is the nuclear Larmor frequency, and T_{1e} is the electron spin-lattice relaxation time. The spin-diffusion constant depends on the mean ^{13}C-^{13}C distance, $r_{^{13}C\text{-}^{13}C}$,[38]

$$D\cong 0.15\frac{\gamma^2\hbar}{r_{^{13}C\text{-}^{13}C}} \tag{6}$$

resulting in $D\cong 3.9\times10^{-13}$ cm^2/s for film A, $D\cong 0.85\times10^{-13}$ cm^2/s for film B, and $D\cong 3.1\times10^{-13}$ cm^2/s for film C. Since T_{1e} is unknown, only the maximum value of ρ can be obtained from (5) by assuming $\omega_n T_{1e}=1$, which yields $\rho_{max}\cong 0.8$ nm for films A and C and $\rho_{max}\cong 1.1$ nm for film B. Comparing these values with the measured distances between paramagnetic sites (R_{ev} and R_{es} in Table I) indicates that the VSD limit does not apply for diamond films studied in this work. This conclusion is supported by the experimental data (see Fig. 5) which indicate that the relaxation follows the single exponential behavior given by Eq. (3) with $n=1$ reasonably well. It is also noted that the equilibrium magnetization value obtained from this fit agreed well with that expected from the measurement of an intensity standard (M_S). An attempt to fit the same data using Eq. (3) with $n=0.5$ yielded an unrealistic value of M_0 that corresponded to a much larger sample. Also, a poor fit was obtained by using $n=0.5$ and a fixed value $M_0=M_S$ (see dashed line in Fig. 5). This relaxation behavior differs from that previously reported for industrial synthetic diamond powders, where relaxation with $n=0.5$ was reported.[12] Several explanations for this discrepancy should be considered: (i) in Ref. 12 MAS was purposely used in order to suppress spin diffusion and create a model system of noncommunicating spins; (ii) a larger concentration of paramagnetic centers was observed in industrial samples, including ferromagnetic inclusions revealed by the reported magnetism of these samples and strongly increased NMR linewidth; (iii) a relatively short time period ($t\ll T_1^c$) was covered in the previous study.

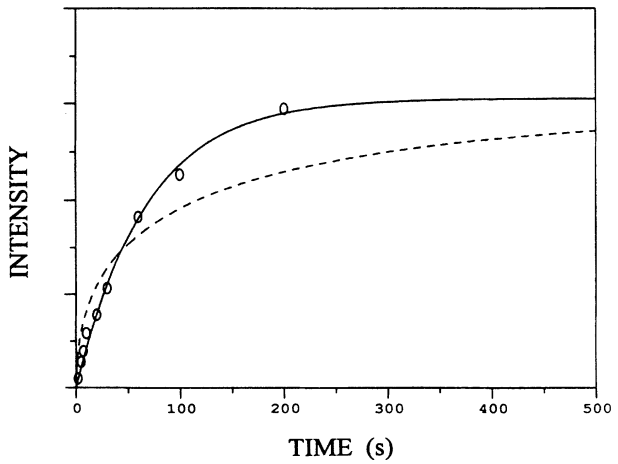

FIG. 5. ^{13}C signal intensity vs time in the progressive saturation experiment. The solid and dashed curves represent least-square fits to Eq. (3) with $n=1$ and $n=0.5$, respectively.

Since in the remaining limiting cases (CSD and LSD) $T_1{}^c$ is proportional to $(N_eD)^{-1}$, the ratio of the relaxation times between the two films studied can now be estimated and compared with the experimental result. Assuming a uniform distribution of paramagnetic centers within the diamond, a T_1^c ratio of 1:1.3:4.5 is predicted for samples A, C, and B, ^{13}C content of 1.1%, 50%, and 100%, respectively, whereas the experimental result is 1:2:8. Although the agreement is only qualitative, it shows that spin diffusion contributes to relaxation in diamond films. An alternative model with the paramagnetic centers concentrated primarily on the crystallite faces is incompatible with the results of this study for several reasons. If the paramagnetic centers were confined to the crystallite surfaces only, then (a) assuming the crystallite size from Table I, there is insufficient time for the spin diffusion to transport carbon magnetization toward the surface of a crystallite (in three-dimensional diffusion the mean displacement during time t is given by $\langle(\mathbf{r}_1-\mathbf{r}_2)^2\rangle=6Dt$. Therefore, during time T_1^c the ^{13}C magnetization is transported over a distance of $\sqrt{DT_1^c}\approx 0.05$ μm in all samples). (b) A nonexponential decay of magnetization would be expected, and (c) the discrepancy between the R_{es} values would be difficult to explain.

F. Distribution of the paramagnetic centers

As claimed in the Introduction above, the conclusion that the distribution of paramagnetic centers is homogeneous is very significant. If they are embedded in the tetrahedral network, a determination of their structure is required, and is not obvious. While a dangling bond may easily be envisioned in the distorted tetrahedral network of amorphous C (a-C) or Si (a-Si), that is not the case in the ordered network found in the thin diamond films. For example, a carbon vacancy would probably result in a spinless pairing of the four sp^3 electron orbitals directed towards the vacancy. If the dangling bonds are not isolated centers embedded in the tetrahedral network, then one may speculate that they are located on the internal surfaces of nanovoids which are embedded in the crystallites. Such nanovoids may possibly be as small as a divacancy or trivacancy, and perhaps viewed as such a complex of dangling bonds partially passivated by H atoms or methyl groups. This picture then implies that the system of these nanovoids is sufficiently dense so that the distribution of the dangling bonds appears homogeneous on the length scale probed by the spin diffusion of the ^{13}C nuclei. If neither of these scenarios can be established,

the possibility that these paramagnetic centers are *not* carbon dangling bonds would clearly have to be considered. Finally, we note that H atoms located in nanovoids and in proximity to dangling bonds would be unobservable by NMR. The postulated nanovoids and microvoids are plausible for another reason as well. The average crystallite size calculated from the ^{1}H NMR spin count assuming coverage of surfaces by hydrogen is ~ 0.2 and ~ 0.7 μm for samples *A* and *B*, respectively. Yet the top crystallities in sample *B* are up to 15 μm across. That would imply that the crystallites growing at the early and intermediate stages of the deposition process would be unreasonably small. A potential resolution of this problem might be such a system of internal nanovoids and microvoids in which the carbon dangling bonds are nearly, but not totally, terminated by H atoms. The H atoms which are sufficiently far from the remaining dangling bonds would then contribute to the observed ^{1}H NMR.

IV. SUMMARY

Using ^{1}H NMR, hydrogen concentrations below 0.6 at. % were determined for the diamond films. The observed hydrogen resonances had linewidths in the 50–65-kHz range and represented rigid hydrogen of high concentration which stabilizes crystalline phases. We exclude the presence of significant concentrations of methyl groups, adsorbed water, trapped methane molecules, and isolated hydrogen atoms in the diamond films studied in this work.

^{13}C NMR measurements indicated that over 99.5% of all carbon in the thin diamond films resides in a quaternary diamondlike environment. Similarly, the only carbon detected in the CP/MAS experiment was found to be in a diamondlike configuration. Also, ^{13}C NMR relaxation measurements were performed on each film. The decay of magnetization could be fitted to an exponential function with a T_1 of 8, 17, and 65 s for films with ^{13}C concentration of 100% 50%, and 1.1%, respectively. The dramatic increase in the ^{13}C relaxation rate of the diamond films, by four orders of magnitude versus that of natural diamond, implies that the dominant relaxation mechanisms is spin diffusion to paramagnetic centers, whose density is $\sim 4\times 10^{17}$ per g (~ 8 ppm). Finally, analysis of the measured relaxation rates indicates that paramagnetic centers are uniformly distributed within the diamond crystallites, at least within the resolution of the ^{13}C spin-diffusion length $\sqrt{DT_1^c} \sim 0.05$ μm. This result is very significant if the paramagnetic centers are carbon dangling bonds, because it is difficult to envision such a dangling bond in an otherwise regular ordered tetrahedral network. It therefore raises the specter of dangling bonds located at the internal surfaces of nanovoids, possibly as small as a divacancy or trivacancy complexes. As the distribution would be homogeneous to within ~ 0.05 μm, their content would be sufficient to strongly impact the electronic and mechanical properties of these films. The scenario of nanovoids and microvoids may also help explain the large discrepancy between the average crystallite size calculated from the ^{1}H NMR spin count and the observed crystallite sizes which are several microns across. While this discrepancy is partially accountable by a high content of small crystallites at the bottom and intermediate layers of the films, the required average of 0.2 and 0.7 μm would entail a large fraction of unreasonably small crystallites. The possibility that a significant fraction of the hydrogen is residing in internal nanovoids and microvoids should, therefore, be seriously considered. This scenario is, however, clearly speculative and additional results are required for its confirmation or refutation.

ACKNOWLEDGMENTS

The authors are indebted to Dr. B.C. Gerstein of the Iowa State University Chemistry Department for invaluable advice and to M.J. Robertson for his assistance with the FT-IR measurement. One of the authors (S.H.) wishes to acknowledge the financial support from the Phillips Petroleum Company. This research was supported at Ames Laboratory by the U.S. Department of Energy, Office of Basic Energy Sciences, Division of Chemical Sciences, under Contract No. W-7405-Eng-82.

[1] J. C. Angus and C. C. Hayman, Science **241**, 919 (1988).

[2] *Diamond, Silicon Carbide, and Related Wide Bandgap Semiconductors,* edited by J. T. Glass, R. Messier, and N. Fujimori, MRS Symposia Proceedings No. 162 (Materials Research Society, Pittsburgh, 1990).

[3] F. P. Bundy, H. T. Hall, H. M. Strong, and R. H. Wentorf, Nature **176**, 51 (1955).

[4] *Wide Bandgap Semiconductors,* edited by T. D. Moustakas, J. I. Pankove, and Y. Hamakawa, MRS Symposia Proceedings No. 242 (Materials Research Society, Pittsburgh, 1992).

[5] R. C. DeVries, Annu. Rev. Mater. Sci. **17**, 161 (1987).

[6] H. Jia, J. Shinar, D. P. Lang, and M. Pruski, Phys. Rev. B **48**, 17 595 (1993).

[7] K. M. McNamara and K. K. Gleason, J. Appl. Phys. **71**, 2884 (1992), and references therein.

[8] K. M. McNamara, K. K. Gleason, D. J. Vestyck, and J. E. Butler, Diamond Rel. Mater. **1**, 1145 (1992).

[9] K. M. McNamara, D. H. Levy, K. K. Gleason, and C. J. Robinson, Appl. Phys. Lett. **60**, 580 (1992).

[10] T. R. Anthony, in *Diamond, Silcon Carbide, and Related Wide Bandgap Semiconductors* (Ref. 2), p. 61.

[11] K. M. McNamara, K. K. Gleason, and C. J. Robinson, J. Vac. Sci. Technol. A **10**, 3143 (1992).

[12] P. M. Henrichs, M. L. Cofield, R. H. Young, and J. M. Hewitt, J. Magn. Reson. **58**, 85 (1984).

[13] W. F. Banholzer and T. R. Anthony, Thin Solid Films **212**, 1 (1992).

[14] Ch. Wild, N. Herres, and P. Koidl, J. Appl. Phys. **68**, 973 (1990).

[15] E. O. Stejskal and J. J. Schaefer, J. Magn. Reson. **18**, 560 (1975).

[16] D. Michel, *Grundlagen und Methoden der Kernmagnetischen Resonanz* (Akademie-Verlag, Berlin, 1979).

[17] M. Pruski, D. K. Sanders, T. S. King, and B. C. Gerstein, J.

Magn. Reson. **96**, 574 (1992).
[18]A. Abragam, *Principles of Nuclear Magnetism* (University Press, Oxford, 1961) Chap. IV.
[19]John F. Nicholas, An Atlas of Models of Crystal Surfaces (Gordon and Breach, New York, 1965).
[20]Y. L. Yang, L. M. Struck, L. F. Sutcu, and M. P. D'Evelyn, Thin Solid Films **225**, 203 (1993).
[21]S. J. Harris and A. M. Weiner, J. Appl. Phys. **67**, 6520 (1990).
[22]N. Bloembergen, E. M. Purcell, and R. V. Pound, Phys. Rev. **73**, 679 (1948).
[23]H. S. Gutowsky and G. E. Pake, J. Chem. Phys. **18**, 162 (1950).
[24]G. Davies, in *Chemistry and Physics of Carbon,* edited by P. L. Walker, Jr., and P. A. Thrower (Dekker, New York, 1977), Vol. 13, pp. 2–128.
[25]W. Kaiser and W. L. Bond, Phys. Rev. **115**, 857 (1959).
[26]M. Lax and E. Burstein, Phys. Rev. **97**, 39 (1955).
[27]R. P. Chin, J. Y. Huang, Y. R. Shen, T. J. Chuang, H. Seki, and M. Buck, Phys. Rev. B **45**, 1522 (1992).
[28]A. V. Hamza, G. D. Kubiak, and R. H. Stulen, Surf. Sci. **206**, L833 (1988).
[29]M. J. Duijvestijn, C. van der Lugt, J. Smidt, R. A. Wind, K. W. Zilm, and D. C. Staplin, Chem. Phys. Lett. **102**, 25 (1983).
[30]H. Lock, G. E. Maciel, and C. E. Johnson, J. Mater. Res. **7**, 2791 (1992).
[31]D. Michel, *Grundlagen und Methoden der Kernmagnetischen Resonanz* (Ref. 16), Chap. IX.
[32]G. R. Khutsishvili, Usp. Fiz. Nauk **87**, 211 (1965) [Sov. Phys. Usp. **8**, 743 (1965)].
[33]M. Goldman, Phys. Rev. A **138**, 1675 (1965).
[34]G. R. Khutsishvili, Zh. Eksp. Teor. Fiz. **42**, 1307 (1962) [Sov. Phys. JETP **15**, 906 (1962)].
[35]H. E. Rorschach, Jr., Physica **30**, 38 (1964).
[36]R. A. Wind, A. Jurkiewica, and G. E. Maciel, Fuel **68**, 1189 (1989).
[37]N. Blombergen, Physica **15**, 386 (1949).
[38]I. J. Lowe and S. Gade, Phys. Rev. **156**, 817 (1967).

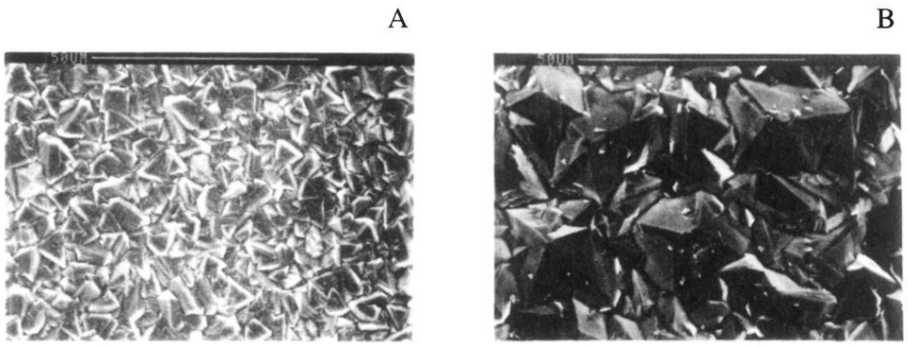

FIG. 1. Scanning electron micrographs of diamond films *A* and *B*.